Inorganic Chemistry

Article

pubs.acs.org/IC

Synthesis and Reactivity of Tripodal Complexes Containing Pendant Bases

Johanna M. Blacquiere,*[,†,‡] Michael L. Pegis,[†] Simone Raugei,[§] Werner Kaminsky,[†] Amélie Forget,[†] Sarah A. Cook,[⊥] Taketo Taguchi,[⊥] and James M. Mayer*[,†]

[†]Department of Chemistry, University of Washington, Box 351700, Seattle, Washington 98195-1700, United States

[‡]Department of Chemistry, University of Western Ontario, London, Ontario N6A 5B7, Canada

[§]Physical Sciences Division, Pacific Northwest National Laboratory, P.O. Box 999, K2-57, Richland, Washington 99352, United States

[⊥]Department of Chemistry, University of California—Irvine, 1102 Natural Sciences II, Irvine, California 92697, United States

Supporting Information

ABSTRACT: The synthesis of a new tripodal ligand family that contains tertiary amine groups in the second-coordination sphere is reported. The ligands are tris(amido)amine derivatives, with the pendant amines attached via a peptide coupling strategy. They were designed to function as new molecular catalysts for the oxygen reduction reaction (ORR), in which the pendant acid/base group could improve the catalyst performance. Two members of the ligand family were each metalated with cobalt(II) and zinc(II) to afford trigonal-monopyramidal complexes. The reaction of the cobalt complexes $[\mathbf{Co(L)}]^-$ with dioxygen reversibly generates a small amount of a cobalt(III) superoxo species, which was characterized by electron paramagnetic resonance (EPR) spectroscopy. Protonation of the zinc complex $Zn[N\{CH_2CH_2NC(O)CH_2N(CH_2Ph)_2\}_3)]^-$ ($[\mathbf{Zn(TN^{Bn})}]^-$) with 1 equiv of acid occurs at a primary-coordination-sphere amide moiety rather than at a pendant basic site. The addition of excess acid to any of the complexes $[\mathbf{M(L)}]^-$ results in complete proteolysis and formation of the ligands $\mathbf{H_3L}$. These undesired reactions limit the use of these complexes as catalysts for the ORR. An alternative ligand with two pyridyl arms was also prepared but could not be metalated. These studies highlight the importance of the stability of the primary-coordination sphere of ORR electrocatalysts to both oxidative *and* acidic conditions.

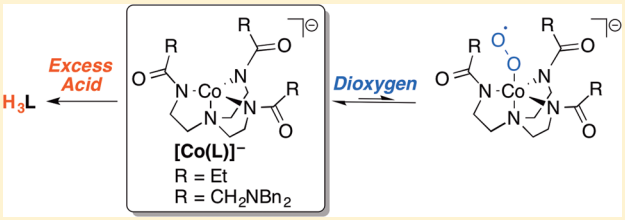

INTRODUCTION

Efficient catalysis of proton−electron-transfer reactions is of increasing importance, especially for the interconversion of chemical and electrical energies. Key examples include the hydrogenase reaction, $2e^- + 2H^+ \rightleftarrows H_2$, and the oxygen reduction reaction (ORR), $O_2 + 4e^- + 4H^+ \rightarrow 2H_2O$. The ORR is the cathode reaction in most fuel cells.[1,2] Platinum is the current state-of-the-art catalyst for the ORR, but its limitations in expense and performance are stimulating much work in this area. While the eventual technological solutions will likely be heterogeneous electrocatalysts, the study of molecular catalysts holds promise to provide new insight into these complex reactions.[3] An ORR catalyst, for instance, has nine substrate units per turnover ($O_2 + 4e^- + 4H^+$), so catalytic cycles have many intermediates, whose identities can be studied using a molecular catalyst. Identification of the intermediates and construction of the structure−activity/selectivity relationships of molecular ORR catalysts will inform design criteria for heterogeneous systems.

Studies of molecular hydrogenase catalysts have shown great value in incorporating "proton relays" in the second-coordination sphere of the metal. These facilitate proton transfer between the active site and the bulk solution and can have other roles. DuBois, Rakowski-DuBois, Bullock, Helm, and co-workers have extensively developed phosphine ligands with pendant, noncoordinating amine groups that dramatically increase the rates of electrocatalytic proton reduction and dihydrogen oxidation relative to analogues without pendant proton shuttles.[4−7] Related ligands have recently been shown to be valuable in nitrogen reduction chemistry.[8] Unfortunately, phosphine−amine ligands do not appear to be compatible with the oxidizing nature of the ORR, as shown by Yang et al. with nickel complexes[9] and later by Tronic et al. with ruthenium compounds.[10,11] Nocera and co-workers earlier developed a family of "hangman" porphyrins and corroles that poise a single carboxylic acid group above the metal center.[12,13] We later extended this approach to simpler iron porphyrin systems with multiple pendant carboxylic acid or pyridinium groups.[14,15] In both cases, the addition of a pendant acid/base group improved the selectivity of the ORR toward $4e^-$ versus $2e^-$ reduction. The porphyrin and corrole systems have some disadvantages, however, including synthetic accessibility, overpotential for the ORR, and often limited stability under oxidizing conditions.

These examples illustrate that there is a need for new ligand types with pendant acid/base functionalities because they show

Received: June 9, 2014
Published: August 8, 2014

   dx.doi.org/10.1021/ic5013389 | Inorg. Chem. 2014, 53, 9242−9253

promise for improving both the rate and selectivity of multi-H^+/e^--transfer reactions. Such ligands should support complexes of abundant and inexpensive first-row transition metals that are coordinatively unsaturated in order to allow substrate binding. The ligands and complexes should be stable to oxidative and acidic conditions. The synthetic route should facilitate systematic ligand variation for both catalyst optimization and mechanistic studies. Herein we report a new tripodal ligand class and several metal complexes of these ligands that satisfy many but not all of these requirements. While our focus has been on new electrocatalysts for the ORR, the design principles and challenges uncovered in this study should be relevant to the development of proton-relay catalysts for other processes as well.

Molecular catalysts for the ORR have focused on porphyrins,[12,16−20] corroles,[13,21] or similar macrocycles.[22,23] These have taken inspiration from biological oxygenase enzymes such as cytochromes P450 and cytochrome *c* oxidase.[24,25] One recent study used tris(2-pyridylmethyl)amine (TPA) ligands with pendant primary amine or amide groups.[26] While several of the synthetic systems are successful at electrochemical or chemical dioxygen reduction, no one system demonstrates high turnover frequencies, high selectivity, low overpotentials, and long-term stability. Tripodal ligands[27−30] have gained attention in both electrochemical[26,31] and chemical[32,33] studies of dioxygen reduction and dioxygen binding. A number of tripodal systems have incorporated pendant hydrogen-bonding and/or acid/base functionalities.[29,34−43] In particular, such ligand systems have been shown to stabilize reactive intermediates that could be derived from dioxygen, such as metal−oxo, hydroxo, and hydroperoxo complexes.[33,40,44−56] An open site for dioxygen binding is available with complexes that have sufficiently bulky ligands that stabilize the coordinatively unsaturated trigonal-monopyramidal geometry. Herein we report the design and synthesis of a tris(2-aminoethyl)amine (tren)-based ligand manifold and coordination to both cobalt and zinc ions (Figure 1). The

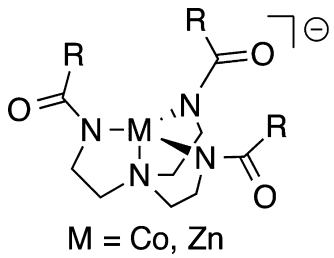

Figure 1. Generic structure of the tren-based metal complexes studied herein [R = Et, $CH_2N(CH_2Ph)_2$].

modular ligand framework was designed to facilitate systematic tuning of the catalyst structure to achieve optimal properties for proton shuttling and selectivity (i.e., through modification of the basicity and bulk of the pendant group). Reactivity with dioxygen is described, but these complexes demetallate under acidic conditions. We discuss the implications of these results to new ligand designs for catalysis of proton/electron-transfer reactions and describe one second-generation ligand.

RESULTS

Synthesis of the Ligands. New ligands have been prepared by the addition of amine-containing groups to tren via a peptide coupling strategy (Scheme 1).[57] Alkylation[58] of

Scheme 1. Synthetic Procedure for the Synthesis of Tertiary Amine-Containing Pro-ligand $H_3(TN^{Bn})$[a]

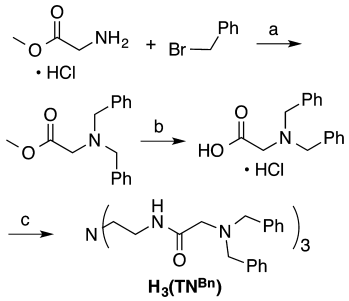

[a]Conditions: (a) $NaHCO_3$, THF/DMSO, 60 °C, 19 h (86% yield); (b) (1) LiOH, MeOH/H_2O, 60 °C, 18 h, (2) HCl (90% yield); (c) (1) NEt_3, NHS, EDAC, CH_2Cl_2, (2) tren, 24 °C, 6 days (84% yield).

methyl-protected glycine with benzyl bromide affords a tertiary amine moiety in high yields (ca. 86%; Scheme 1a). Deprotection[59] of the methyl ester is followed by amide bond formation, which is facilitated by activation with *N*-hydroxysuccinimide (NHS) and 1-ethyl-3-[3-(dimethylamino)-propyl]carbodiimide hydrochloride (EDAC) as the coupling agent (Scheme 1b,c). This route affords the protonated ligand (or pro-ligand) $H_3(TN^{Bn})$ in an overall yield of 65%. The pro-ligand was characterized by ^1H and $^{13}C\{^1H\}$ NMR and IR spectroscopies and by high-resolution mass spectrometry (HR-MS). By ^1H NMR spectroscopy, as expected, only four unique signals are observed for the distinct methylene moieties. The benzyl methylene signals (δ = 3.59 ppm, $CDCl_3$) integrate in a 2:1 ratio to each of the tren backbone methylene resonances. The symmetry and integration data both confirm that all three tren arms are functionalized. The amide N−H resonance is obscured by the aromatic signals of the benzyl groups, but its shift of δ = 7.21 ppm ($CDCl_3$) is indicated by correlation to the adjacent methylene group (δ = 3.21 ppm, $CDCl_3$) in the $^1H-^1H$ COSY NMR spectrum. The IR stretching frequencies at 3370 and 1669 cm^{-1} are diagnostic for the respective NH and CO moieties of the amide functionality.[60]

A "control ligand" without the pendant tertiary amine functionality was readily accessible by reacting tren with propionyl chloride. The resulting pro-ligand $H_3(TEt)$ was isolated by flash chromatography in moderate yield (Scheme 2) and characterized by ^1H and ^{13}C NMR and IR spectroscopies and HR-MS.

Scheme 2. Synthesis of a tren-Based "Control" Ligand, $H_3(TEt)$[a]

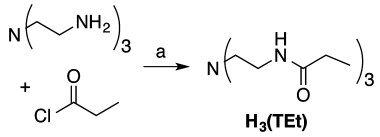

[a]Conditions: (a) NEt_3, CH_2Cl_2, 0−24 °C, 21 h (38% yield).

A tren-based ligand with an aryl-substituted pendant amine was synthesized in a similar manner to $H_3(TN^{Bn})$ (Scheme 3). The tertiary amine compound, 2-[*N*-methyl-*N*-(phenylamino)]benzoic acid, was easily accessed in two steps following modified literature procedures.[61] To achieve high yields in the tren coupling step, it proved essential to isolate and extensively dry the NHS-activated carboxylate intermedi-

dx.doi.org/10.1021/ic5013389 | Inorg. Chem. 2014, 53, 9242−9253

Scheme 3. Synthesis of an Aryl-Substituted Tertiary Amine-Containing Pro-ligand, $H_3(TN^{Ph})$[a]

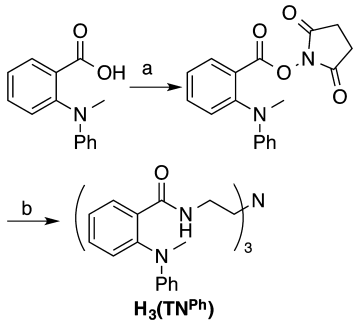

[a]Conditions: (a) NHS, EDAC, CH_2Cl_2, 24 °C, 6 h (84% yield); (b) tren, CH_2Cl_2, 40 °C, 3 h (90% yield).

ate. The target aryl-substituted pro-ligand $H_3(TN^{Ph})$ was synthesized in four steps with an overall yield of 48%. Amide bond formation at all three ligand arms was confirmed by integration of the ^1H NMR spectrum.

One additional ligand with pyridyl donors in place of two amide donors was prepared in an attempt to avoid the protic instability of the amide-based complexes that will be discussed below. $H(py_2N^{Bn})$ was synthesized using a (2-aminoethyl)bis-(2-pyridylmethyl)amine core rather than tren (Scheme 4). The

Scheme 4. Synthesis of the Tripodal Ligand with Two Pyridyl Donors, $H(py_2N^{Bn})$[a]

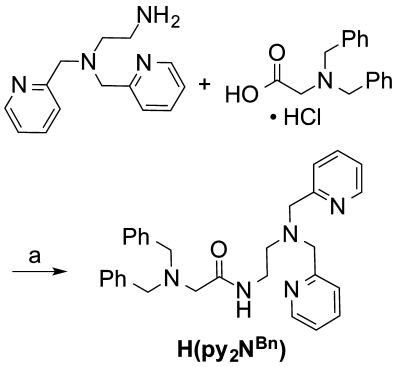

[a]Conditions: (a) hydroxybenzotriazole, DCC, CH_2Cl_2, NEt_3, 24 °C, 72 h (34% yield).

tripodal starting material was synthesized according to literature procedures[62] and was coupled to *N,N*-dibenzylglycine hydrochloride using a peptide coupling strategy. Formation of the target compound was confirmed by ^1H and ^{13}C NMR and IR spectroscopies and HR-MS.

Preparation and Physical Properties of the Tripodal Cobalt and Zinc Complexes. Treatment of the pro-ligand $H_3(TN^{Bn})$ with excess KH in *N,N*-dimethylformamide (DMF) rapidly produced bubbles, which is indicative of dihydrogen evolution and K_3L salt formation (Scheme 5). Deprotonation of the amide was supported by the absence of a correlation from the adjacent methylene group in the $^1H-^1H$ COSY NMR spectra of NMR-scale reactions. In preparative-scale reactions, the deprotonated ligand was subsequently treated with anhydrous $CoCl_2$ to afford the desired product $K[Co(TN^{Bn})]$. The KCl salt byproduct was removed via filtration, and the product was isolated in moderate yield (43%) by precipitation with Et_2O. $K[Co(TN^{Bn})]$ has low solubility in all solvents

Scheme 5. Synthesis of Pendant Amine-Containing Complex $NEt_4[Co(TN^{Bn})]$[a]

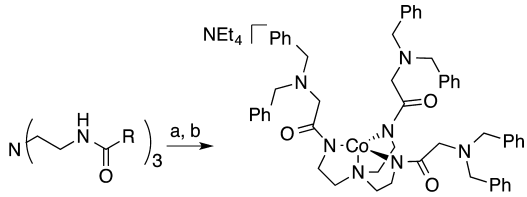

[a]Conditions: (a) (1) KH, DMF, (2) $CoCl_2$ (43% yield); (b) NEt_4Cl, CH_3CN (39% yield).

except DMF (vide infra) but is converted to a more soluble derivative, $NEt_4[Co(TN^{Bn})]$, upon stirring with NEt_4Cl in MeCN (Scheme 5b). The complex $NEt_4[Co(TEt)]$ (Chart 1),

Chart 1. Tripodal Cobalt and Zinc Complexes Explored in This Report

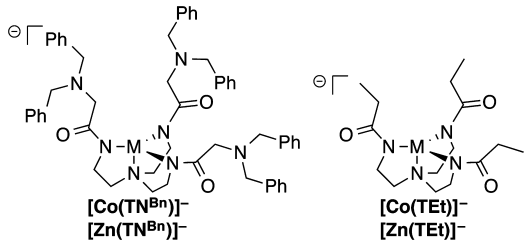

without a pendant amine functionality, was obtained in an analogous manner. Formation of these salts, designated as $NEt_4[Co(L)]$, was confirmed by structural determination via X-ray crystallography and a combination of ^1H NMR, UV−vis, and electron paramagnetic resonance (EPR) spectroscopies and mass spectrometry (MS).[63] Unfortunately, we were unable to obtain cobalt complexes of the ligands $(py_2N^{Bn})^-$ and $(TN^{Ph})^{3-}$. Synthetic routes to the latter were not pursued in detail because it was judged that the lower basicity of the second-coordination-sphere arylamines would exacerbate the problems identified below.

Diamagnetic derivatives $K[Zn(L)]$ were synthesized in a similar manner for L = $(TN^{Bn})^{3-}$ and $(TEt)^{3-}$ (Chart 1). ^1H NMR analyses of $K[Zn(TN^{Bn})]$ and $K[Zn(TEt)]$ revealed small but significant shifts in the ligand resonances relative to the pro-ligands, most notably in the methylene unit adjacent to the amide N−H, which shifts 0.07 and 0.12 ppm downfield from the pro-ligand in the respective complexes [δ, DMF-d_7: 3.36/3.29 for $K[Zn(TN^{Bn})]/H_3(TN^{Bn})$; 3.32/3.20 for $K[Zn(TEt)]/H_3(TEt)$]. $^1H-^1H$ COSY NMR analysis showed no correlation from this signal to an N−H resonance, confirming that the ligand is in a trianionic form.

The pro-ligand $H(py_2N^{Bn})$ was similarly treated with KH and $ZnCl_2$ in an attempt to synthesize $[Zn(py_2N^{Bn})]Cl$. ^1H NMR analysis of crude reaction mixtures confirmed complete reaction of the pro-ligand, but the complexity of the spectrum indicated that a mixture of products was generated. Attempts to selectively crystallize the desired complex were not achieved despite several attempts with different counterions (e.g., $[B(3,5-(CF_3)_2C_6H_3)_4]^-$, NO_3^-, BF_4^-, OTf^-, and PF_6^-). Similar isolation challenges were encountered upon using $CoCl_2$ or $FeCl_2$ as the metal precursor. Alsfasser et al. have acknowledged that for related dipyridylamido tripodal ligands the observed coordination environment is highly dependent on the ancillary

dx.doi.org/10.1021/ic5013389 | Inorg. Chem. 2014, 53, 9242−9253

Table 1. Summary of the Experimental Data for the Tripodal Complexes

	$[Co(TEt)]^-$	$[Co(TN^{Bn})]^-$	$[Zn(TEt)]^-$	$[Zn(TN^{Bn})]^-$
λ_{max}, nm (ε, M^{-1} cm^{-1})	404 (30), 584 (100), 609 (93)	412 (31), 588 (104), 614 (103)		
$[M]^-$ obsd (expected), m/z[a]	370.2 (370.1)	913.5 (913.4)	375.3 (375.1)	918.5 (918.4)
μ_{eff}, BM[b]	4.36	4.21		
g values	3.78[c] (4.28, 2.00)[d]	3.83[c] (4.30, 2.00)[d]		
E_{pa}, mV vs $Fc^{0/+}$	109	38		

[a]MALDI MS data. [b]Evans' method performed at 298 K. [c]EPR data collected at 77 K. [d]EPR data collected at 10 K.

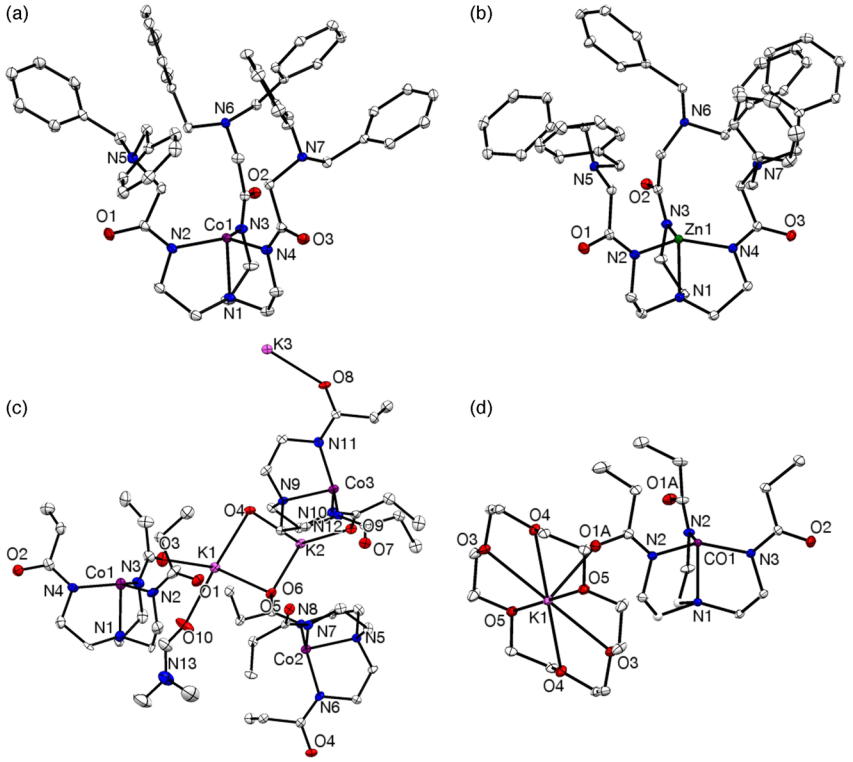

Figure 2. Thermal ellipsoid diagrams of (a) $NEt_4[Co(TN^{Bn})]$, (b) $NEt_4[Zn(TN^{Bn})]$, (c) $K_3[Co(TEt)]_3 \cdot 2DMF$, in which one DMF molecule has been removed for clarity, and (d) **K(18-c-6)[Co(TEt)]**. The NEt_4 cation is not shown in parts a and b, and hydrogen atoms are not shown. Non-hydrogen atoms are represented by Gaussian ellipsoids at the 30% probability level.

ligands used (i.e., chlorine in our case).[64] Possibly, the use of a metal precursor that contains weakly or noncoordinating anions would lead to a cleaner product distribution.

^{1}H NMR spectroscopy proved to be a reliable tool to confirm formation of the paramagnetic cobalt complexes. The signals are all paramagnetically shifted, with a diagnostic peak at ca. 80 ppm for both $[Co(TN^{Bn})]^-$ and $[Co(TEt)]^-$. For $[Co(TN^{Bn})]^-$, the broad signals at 6.85, 5.74, and 3.69 ppm (DMF-d_7) show that the benzyl signals are significantly less paramagnetically shifted than the tren-backbone methylene units. Evans' method analysis[65] of $[Co(TN^{Bn})]^-$ and $[Co(TEt)]^-$ gave μ_{eff} = 4.21 and 4.36, respectively, consistent with the assignment of both cobalt(II) species as high-spin ($S = {}^3/_2$).

The blue cobalt(II) complexes display three prominent optical features between 400 and 650 nm (Table 1). The energies and intensities of these bands are similar to the features previously observed for related cobalt(II) complexes with trigonal-monopyramidal coordination geometries[27,29,50,57,66] and are assigned as $^4A_2 \rightarrow {}^4A_2$, $^4A_2 \rightarrow {}^4E$, and $^4A_2 \rightarrow {}^4E$ transitions.[66] These results strongly indicate that in solution the blue cobalt complexes are four-coordinate with an open site cis to the three amidate moieties. By comparison, five-coordinate cobalt(II) complexes with trigonal-bipyramidal coordination geometries, in which a solvent molecule acts as an additional axial ligand, are generally pink in color.[27−29,57] $[Co(TN^{Bn})]^-$ and $[Co(TEt)]^-$ retain the blue color in solution, suggesting that the trigonal-monopyramidal geometry persists even when the complexes are dissolved in coordinating solvents such as acetonitrile. This solution behavior is in contrast to the structurally similar amidate-ligated complex reported by Jones and MacBeth, which forms a solvent adduct in MeCN.[27] Their ligand, ($N(o\text{-}PhNHC(O)^iPr)_3$), is analogous to $(TEt)^{3-}$ except that the amide substituent is an isopropyl group rather than ethyl and the ligand backbone is constructed from tris(2-aminoethyl)phenyl(amine) rather than tren. The difference in solution behavior likely results from electronic effects rather than steric effects because the MacBeth ligand has the less σ-donating aryl backbone and the more sterically demanding isopropyl substituents.

The tripodal complexes $[M(TEt)]^-$ and $[M(TN^{Bn})]^-$ were also analyzed by matrix-assisted laser desorption ionization MS (MALDI MS) in negative-ion mode with a polyaromatic hydrocarbon matrix.[67] For each of the cobalt and zinc complexes, the molecular anion was observed with an excellent

dx.doi.org/10.1021/ic5013389 | Inorg. Chem. 2014, 53, 9242−9253

Table 2. Selected Bond Lengths and Angles for the Tripodal Cobalt and Zinc Complexes[a]

	$K_3[Co(TEt)]_3 \cdot 2DMF$	K(18-c-6) [Co(TEt)]	$NEt_4[Co(TN^{Bn})]$	$NEt_4[Zn(TN^{Bn})]$
		Bond Length (Å)		
M−N1	2.090(7)	2.0877(18)	2.0878(12)	2.0915(11)
M−N2	1.955(7)	1.9579(13)	1.9573(13)	1.9672(12)
M−N3	1.979(6)	1.9579(13)[b]	1.9588(12)	1.9718(12)
M−N4	1.928(7)	1.9593(18)	1.9594(13)	1.9665(11)
		Angle (deg)		
N1−M−N2	85.7(3)	85.68(4)	85.88(5)	87.17(5)
N1−M−N3	85.5(3)	85.68(4)	85.22(5)	86.94(5)
N1−M−N4	85.4(3)	84.73(7)	85.81(5)	86.36(4)
N2−M−N3	117.6(3)	118.46(8)	119.60(6)	118.21(5)
N3−M−N4	118.0(3)	119.80(4)	120.93(6)	121.19(5)
N2−M−N4	122.5(3)	119.80(4)	117.74(6)	119.68(5)
τ'	0.89	0.93	0.92	0.93

[a]One of the three Co molecules in the unit cell. [b]Generated by symmetry from Co−N2.

isotope match to the expected composition (Table 1 and Figures S21−S24 in the Supporting Information, SI).

Structural Studies of the Tripodal Cobalt and Zinc Complexes. Structural analyses of **K[Co(TEt)]**, **NEt_4[Co(TN^{Bn})]**, and **NEt_4[Zn(TN^{Bn})]** by X-ray diffraction (XRD) methods show that each member of the series is trigonal monopyramidal in the solid state with roughly C_{3v} symmetry (Figure 2 and Table 2). Kerton and Kozak have proposed τ' as a metric to assess the geometry and distortion in four-coordinate metal complexes, similar to the use of τ for five-coordinate structures.[28] A trigonal-monopyramidal geometry will give $\tau' = 1$, while a tetrahedron gives $\tau' = 1.5$. The τ' values of ca. 0.9 for the complexes reported herein (Table 2) are similar to those of related trigonal-monopyramidal complexes[28] and indicate minimal distortion from the ideal geometry.

In all cases, the equatorial metal−amide bonds are ca. 0.1 Å shorter than the apical metal−amine bond. The structure of **$K[Co(TEt)]^-$** includes three cobalt molecules in the asymmetric unit and two DMF solvent molecules. The potassium ions bridge adjacent **$[Co(TEt)]^-$** species through interactions with the ligand carbonyl oxygen atoms to create an extended structure (Figure 2a). This Lewis acid/base interaction results in a distortion of the primary-coordination sphere, where the potassium-associated amide has a slightly longer Co−N bond by ca. 0.03 Å and, by compensation, a second Co−N bond shortens by the same distance (Table 2). A similar K^+-bridged extended network was observed previously in a cobalt complex with a tren-based cryptand ligand.[57] These observed solid-state interactions are likely the origin of the limited complex solubility. In support of this view, crystallization of **K[Co(TEt)]** in the presence of 18-crown-6 afforded a salt that is soluble in a broader range of solvents and has a structure with a sequestered potassium ion and a lattice that is devoid of DMF molecules.

EPR Spectral Properties of the Tripodal Cobalt Complexes. The cobalt complexes were analyzed by X-band EPR spectroscopy as frozen solutions at 10 and 77 K in standard perpendicular (⊥) mode. At the higher temperature, both **$[Co(TEt)]^-$** and **$[Co(TN^{Bn})]^-$** displayed a derivative signal at ca. $g = 3.8$ (Table 1) that is consistent with similar high-spin ($S = {}^3/_2$) trigonal-monopyramidal complexes.[68] Broadening of the signals due to spin−lattice relaxation[69] is minimized at 10 K, and two features are observed for each complex with g values at ca. 4.3 and 2.0 (160 and 344 mT, respectively; Figure 3). These features are assigned to $g_\perp$ and $g_\parallel$,

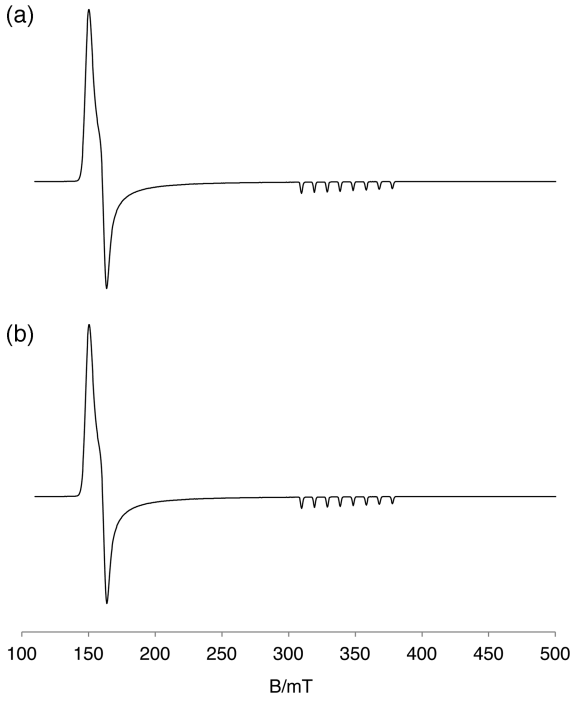

Figure 3. Perpendicular-mode X-band EPR spectra of (a) **$[Co(TN^{Bn})]^-$** and (b) **$[Co(TEt)]^-$**; recorded at 10 K in a 1:1 THF/DMF glass.

respectively (Table 1). The presence of these two features indicates that the complexes have axial symmetry in solution ($E/D \sim 0.0$) and that they retain the C_{3v} symmetry observed in the solid state by XRD. The signal at $g = 2.0$ is split into an eight-line pattern because of the expected hyperfine coupling to the ^{57}Co nucleus ($I = {}^7/_2$). The magnitudes of the hyperfine couplings in **$[Co(TN^{Bn})]^-$** ($A_z = 98 \times 10^{-4}$ cm^{-1}) and **$[Co(TEt)]^-$** ($A_z = 96 \times 10^{-4}$ cm^{-1}) are the same as those found for other cobalt(II) trigonal-bi- or monopyramidal complexes.[50,68,70]

Electrochemical Properties of the Tripodal Cobalt Complexes. Cyclic voltammograms of **$[Co(TEt)]^-$** and **$[Co(TN^{Bn})]^-$** were recorded at a scan rate of 100 mV/s in acetonitrile with a glassy carbon working electrode and ^{n}Bu$_4$N[PF$_6$] as the supporting electrolyte (Figure 4 and Table 1). Both complexes display irreversible oxidations (even at a higher scan rate of 300 mV/s) similar to previously reported cobalt

dx.doi.org/10.1021/ic5013389 | Inorg. Chem. 2014, 53, 9242−9253

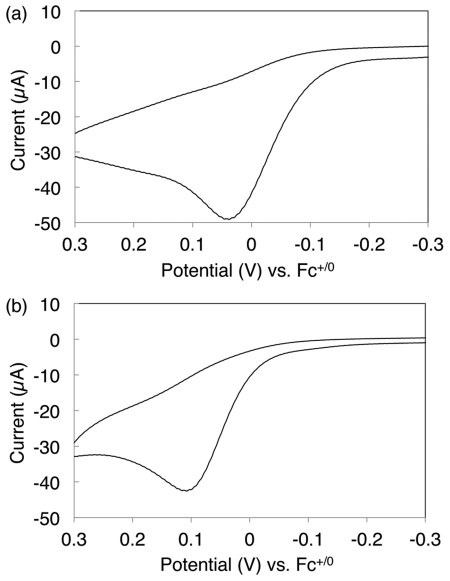

Figure 4. Cyclic voltammograms of (a) $[\mathbf{Co}(\mathbf{TN}^{\mathbf{Bn}})]^-$ and (b) $[\mathbf{Co}(\mathbf{TEt})]^-$ in CH_3CN recorded at a scan rate of 100 mV/s with a glassy carbon working electrode and $^nBu_4N[PF_6]$ as the electrolyte.

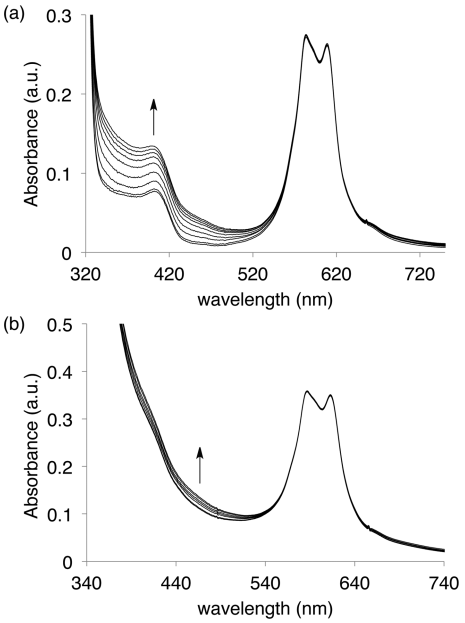

Figure 5. UV−vis spectra of 2.5 mM solutions of (a) $[\mathbf{Co}(\mathbf{TEt})]^-$ and (b) $[\mathbf{Co}(\mathbf{TN}^{\mathbf{Bn}})]^-$ upon the addition of 15 equiv of dioxygen monitored over a 30 min period.

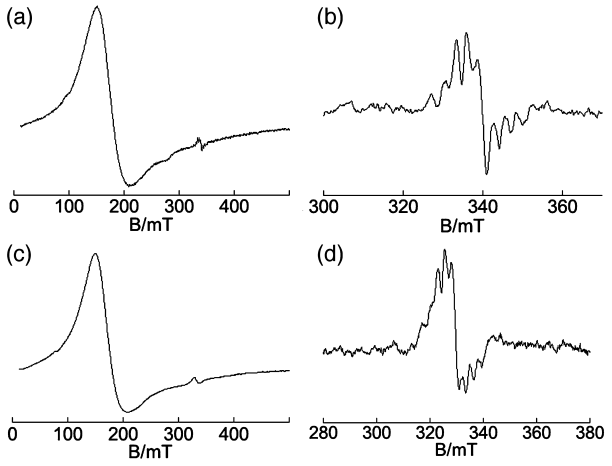

Figure 6. X-band EPR spectra, recorded at 77 K in a 1:1 THF/DMF glass: (a) $[\mathbf{Co}(\mathbf{TEt})]^-$ following dioxygen addition; (b) expansion of the g = 2 region of part a; (c) $[(\mathbf{Co}(\mathbf{TN}^{\mathbf{Bn}})]^-$ following dioxygen addition; (d) expansion of the g = 2 region of part c.

trigonal-monopyramidal complexes.[50,57] This points to the instability of the cobalt(III) complexes with low coordination numbers. The more negative anodic peak potential (E_{pa}) for $[\mathbf{Co}(\mathbf{TN}^{\mathbf{Bn}})]^-$ relative to $[\mathbf{Co}(\mathbf{TEt})]^-$ (E_{pa} = 38 and 109 V vs $Fc^{+/0}$, respectively) could reflect the electron-donating nature of the 3° amine moieties either inductively or by weak coordination with the cobalt(III) product.

Reactivity of the Tripodal Complexes with Dioxygen. The addition of excess dioxygen to solutions of $[\mathbf{Co}(\mathbf{TN}^{\mathbf{Bn}})]^-$ or $[\mathbf{Co}(\mathbf{TEt})]^-$ did not result in any visually observable color change or in the formation of a dioxygen adduct, as judged by MALDI MS. ^1H NMR spectra in DMF-d_7 of the oxygenated solutions did not indicate the formation of a new species, but quantification of the cobalt complexes relative to an internal standard (1,3,5-trimethoxybenzene) revealed minor consumption of $[\mathbf{Co}(\mathbf{TN}^{\mathbf{Bn}})]^-$ (17%) and $[\mathbf{Co}(\mathbf{TEt})]^-$ (10%).

The dioxygen reactivity was probed optically for both $[\mathbf{Co}(\mathbf{TEt})]^-$ and $[\mathbf{Co}(\mathbf{TN}^{\mathbf{Bn}})]^-$ (Figure 5). The addition of excess (15 equiv, 82 μmol) dioxygen to $[\mathbf{Co}(\mathbf{TEt})]^-$ (2.5 mM, 5.6 μmol) resulted in increased absorption at wavelengths below 520 nm over a period of 30 min, but very little change was observed for the features around 600 nm (Figure 4a). Similar behavior is observed for $[\mathbf{Co}(\mathbf{TN}^{\mathbf{Bn}})]^-$ but with a less pronounced change in the absorbance (Figure 5b).

The product of dioxygen reactivity was probed by EPR spectroscopy by bubbling solutions of $[\mathbf{Co}(\mathbf{TEt})]^-$ and $[\mathbf{Co}(\mathbf{TN}^{\mathbf{Bn}})]^-$ with dry dioxygen for 2 min and then cooling to a glass at 77 K (Figure 6). Minor formation of a new species is evident with both complexes by the appearance of a new signal at ca. g = 2 with eight-line hyperfine coupling to cobalt ($I = {}^7/_2$): $A_z = 28 \times 10^{-4}$ cm^{-1} for $[\mathbf{Co}(\mathbf{TEt})]^-$ and $A_z = 25 \times 10^{-4}$ cm^{-1} for $[\mathbf{Co}(\mathbf{TN}^{\mathbf{Bn}})]^-$. The location of the signal and magnitude of the coupling are consistent with the formation of a cobalt(III) superoxo adduct.[71,72] The signal at g = 2 disappears upon sparging of the thawed oxygenated solution with dinitrogen, indicating that the formation of the cobalt(III) superoxo complexes is reversible. The superoxo signal was not observed at 10 K because of obstruction by $g_{||}$ of the parent species. To obtain additional insight into the dioxygen adduct of $[\mathbf{Co}(\mathbf{TN}^{\mathbf{Bn}})]^-$, some computational studies were performed as described in the Discussion section.

Reactivity of the Tripodal Complexes with Acid. The diamagnetic complex $[\mathbf{Zn}(\mathbf{TN}^{\mathbf{Bn}})]^-$ was treated with 1 equiv of the acid [H-DMF]OTf in either DMF-d_7 or CD_3CN under anaerobic conditions, and the reaction was analyzed by ^1H NMR spectroscopy (Figure 7a,b). Only minor amounts of the starting material $[\mathbf{Zn}(\mathbf{TN}^{\mathbf{Bn}})]^-$ remain (ca. 5% relative to the internal standard); signals that match the pro-ligand $\mathbf{H_3}(\mathbf{TN}^{\mathbf{Bn}})$ are found in ca. 25% yield. The remaining 70% of material is tentatively assigned as a protonated species. The site of protonation was identified through $^1H-^1H$ COSY NMR analysis, where a correlation between H^b and a new signal was observed that strongly suggests that the site of protonation is the adjacent amide moiety. Protonation of the tertiary amine was not observed, which would have been indicated by

dx.doi.org/10.1021/ic5013389 | Inorg. Chem. 2014, 53, 9242−9253

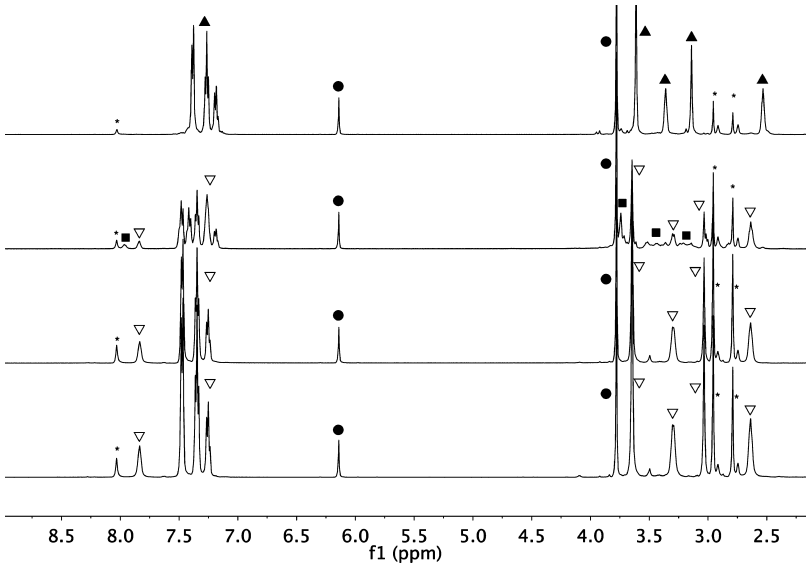

Figure 7. Protonation study with $\mathbf{K[Zn(TN^{Bn})]}$ in DMF-d_7: (a) mixture of $\mathbf{K[Zn(TN^{Bn})]}$ (▲) and an internal standard (●); (b) addition of 1 equiv of [H-DMF]OTf; (c) addition of 3 equiv of [H-DMF]OTf; (d) sample from part c spiked with 0.5 equiv of authentic $\mathbf{H_3(TN^{Bn})}$ (▽). Internal standard = 1,3,5-trimethoxybenzene. Signal intensities are normalized to a set height for the internal standard. DMF, from both residual proteo solvent molecules and added [H-DMF]OTf, is identified by *, and unassigned signals are identified by ■.

correlations from both methylene units H^c and H^d (see Figure 8). Expected correlations were observed between the methylene units of the tren backbone (H^a and H^b; Figure 8).

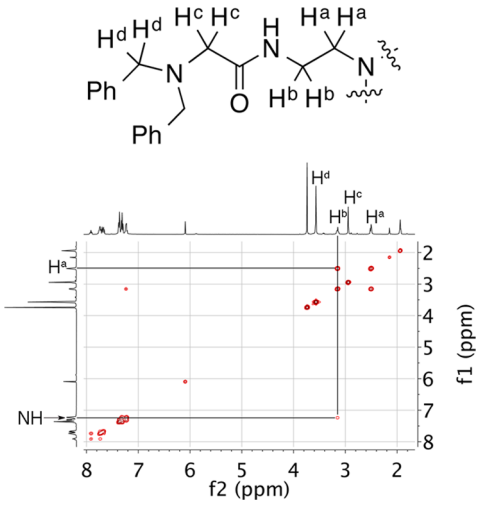

Figure 8. ^{1}H–^{1}H COSY NMR spectrum of a solution of $\mathbf{[Zn(TN^{Bn})]^-}$ + 1 equiv of [H-DMF]OTf in CD_3CN. The structure above is shown for labeling purposes only.

The treatment of $\mathbf{[Zn(TN^{Bn})]^-}$ with weaker acids in CD_3CN with pK_a values ranging from 14 to 27 (cf. pK_a of [HDMF]OTf = 6)[73,74] also afforded the protonated ligand $\mathbf{H_3(TN^{Bn})}$. In the presence of *p-tert*-butylphenol [pK_a(MeCN) = 27], an unassigned intermediate was observed at short reaction times, which mostly converts (over ca. 1 h) to the pro-ligand.

The paramagnetic complex $\mathbf{[Co(TN^{Bn})]^-}$ was titrated with a total of 1 equiv of [H-DMF]OTf, followed by the addition of the strong phosphazine base ^{t}BuP_2(dma) (dma = dimethylamine; *N‴-tert*-butyl-*N*,*N*′,*N*′-tetramethyl-*N*″-[tris(dimethylamino)phosphoranylidene]phosphorimidic triamide). Additions were monitored optically, and the resulting spectra indicate that protonation with a single equivalent of acid is reversible (Figures S25 and S26 in the SI). Optical monitoring of $\mathbf{[Co(TEt)]^-}$ likewise exhibited reversible protonation upon the addition of 1 equiv of acid followed by base (Figures S25 and S26 in the SI).

The addition of a total of 3 equiv of [H-DMF]OTf to $\mathbf{[Zn(TN^{Bn})]^-}$ resulted in the quantitative formation of $\mathbf{H_3(TN^{Bn})}$ (by ^{1}H NMR spectroscopy; Figure 7c). The assignment of this species was confirmed upon spiking the solution with 0.5 equiv of authentic pro-ligand (Figure 7d). Analogous ^{1}H NMR experiments with $\mathbf{[Co(TN^{Bn})]^-}$, $\mathbf{[Zn(TEt)]^-}$, and $\mathbf{[Co(TEt)]^-}$ afforded very similar results, in which the addition of 3 equiv of acid also generates the pro-ligand in quantitative yield (Figures S27–S32 in the SI).

DISCUSSION

Reported herein are new tetradentate nitrogen-donor ligands in which a tren backbone has been coupled to a number of moieties through an amide linkage. Most of our studies have used the $\mathbf{(TN^{Bn})^{3-}}$ ligand in which the subunits are derived from the amino acid glycine, with the amine moiety converted to a tertiary center. In principle, this ligand is modular and versatile because the use of different amino acids or substituents on the amine would afford a range of derivatives. The versatility in the design is demonstrated with the $\mathbf{(TN^{Ph})^{3-}}$ and $\mathbf{(py_2N^{Bn})^-}$ ligands. The former contains an aryl-substituted pendant amine, while the latter retains the pendant *N*-benzyl functionality of $\mathbf{(TN^{Bn})^{3-}}$ but substitutes two of the tripodal arms with pyridyl donors. The control ligand $\mathbf{(TEt)^{3-}}$, without basic groups in the second-coordination sphere, was designed with ethyl groups adjacent to the amide to offer steric protection of the open coordination site in the resulting metal complexes. This protection mimics that of $\mathbf{(TN^{Bn})^{3-}}$, which was expected to form a monometallic cobalt(III) superoxo rather than a μ-peroxodicobalt(III) species upon oxygenation.[51,75]

Cobalt(II) and zinc(II) complexes were prepared with the $\mathbf{(TN^{Bn})^{3-}}$ and $\mathbf{(TEt)^{3-}}$ ligands. The $\mathbf{[Zn(L)]^-}$ complexes act as redox neutral and diamagnetic derivatives that allow ^{1}H NMR

dx.doi.org/10.1021/ic5013389 | *Inorg. Chem.* 2014, 53, 9242–9253

spectroscopy to be employed as a tool to track proton movement. Cobalt was chosen for its synthetic accessibility, and cobalt(II) species are known to reduce dioxygen through either a $4e^-$ or a more common $2e^-$ pathway. This was seen as an opportunity to rigorously test the efficacy of the pendant basic group of $[\mathbf{Co(TN^{Bn})}]^-$ to alter selectivity in the ORR relative to $[\mathbf{Co(TEt)}]^-$. The cobalt complexes with the $(\mathbf{TN^{Bn}})^{3-}$ and $(\mathbf{TEt})^{3-}$ ligands both have four-coordinate, coordinatively unsaturated, trigonal-monopyramidal structures. In $[\mathbf{Co(TN^{Bn})}]^-$, the amine groups are distant from the cobalt(II) center. The two complexes are similar structurally and spectroscopically, displaying expected characteristics for cobalt(II) complexes with this primary-coordination sphere. Values for the structural parameter τ' close to 1 indicate that very little distortion from the expected trigonal-monopyramidal coordination geometry is found in the solid state, and analysis of frozen solutions by EPR spectroscopy points toward C_3-symmetric cobalt(II) species in an axial environment. The blue color of both complexes and UV−vis spectra strongly support the presence of four-coordinate complexes in solution. The data suggest that the primary-coordination spheres of $[\mathbf{Co(TN^{Bn})}]^-$ and $[\mathbf{Co(TEt)}]^-$ are similar and that the former is a reasonable control complex without basic groups in the second-coordination sphere. The zinc derivatives with these ligands appear to be structurally similar, based on the solid-state structure of $[\mathbf{Zn(TN^{Bn})}]^-$ and solution-state NMR analyses, indicating that these are reasonable diamagnetic analogues of the cobalt complexes.

The cobalt derivatives react with dioxygen only to a small extent, with low conversion of $[\mathbf{Co(TN^{Bn})}]^-$ and $[\mathbf{Co(TEt)}]^-$, as evidenced by ^{1}H NMR, EPR, and UV−vis spectroscopies. Related dioxygen adducts have been reported to have intense charge-transfer bands in the UV−vis spectrum, with molar absorptivities of $\varepsilon \sim 10^4$ M^{-1} cm^{-1}.[69,76] In the reactions of dioxygen with $[\mathbf{Co(TN^{Bn})}]^-$ or $[\mathbf{Co(TEt)}]^-$, little depletion of the starting material is observed, but a small amount of product is visible because of its high ε.[77] With the rough assumption that the product ε values are approximately 10^4 M^{-1} cm^{-1}, as observed for octahedral adducts, the equilibrium constants for dioxygen binding would be ca. 10^{-3} atm^{-1} for both compounds. EPR studies indicated that sparging of dioxygen-saturated solutions with dinitrogen results in decoordination of dioxygen to regenerate the trigonal-monopyramidal starting material. The experimental and computational (see below) results are all consistent with equilibrium dioxygen binding to $[\mathbf{Co(TN^{Bn})}]^-$ or $[\mathbf{Co(TEt)}]^-$, which lies strongly in favor of the open-site species (Scheme 6).

The low conversion precludes detailed experimental examination of the dioxygen adducts, so we turned to computational analysis. Density functional theory (DFT) calculations were performed using Thrular's M06L exchange and correlation functional,[78] with the Stuttgart SDD basis set for the cobalt atom, the 6-311G** basis set for dioxygen atoms, and 6-31G for all other atoms (see the SI for additional details). Calculations indicate that an end-on coordination of dioxygen is the most favored structure for the adduct, but the dioxygen binding free energy is endoergic by about +10 kcal mol^{-1} for both $[\mathbf{Co(TN^{Bn})}]^-$ and $[\mathbf{Co(TEt)}]^-$. This thermodynamic bias against dioxygen coordination is qualitatively consistent with the low conversion to the cobalt superoxo complex that was observed experimentally. Quantitatively, the magnitude is higher than anticipated from the experimental K_{eq} values, which is a typical problem for M−O_2 binding energies obtained from DFT calculations.[79,80] The computed Co−O and O−O bond lengths of 1.92 and 1.27 Å are within the ranges of 1.86−1.97 and 1.24−1.30 Å typically observed for the respective distances in reported six-coordinate cobalt(III) superoxo species.[75,81] Relative to molecular oxygen,[75] the O−O bond is only lengthened by ca. 0.06 Å, indicating that charge donation into the dioxygen moiety is small. Characterization as a superoxo ligand is also indicated by the computed Mulliken charges for proximal and distal oxygen atoms of −0.13 and −0.22 e^-, respectively, and corresponding spin charges of 0.39 and 0.63 e^-, respectively. All of these data are consistent with a weak interaction of dioxygen with the metal center. Still, strong dioxygen coordination is not a prerequisite for electrocatalytic dioxygen reduction, as evidenced by Arnold's studies of a tripodal cobalt tris(2-pyridylmethyl)amine complex.[31]

These species are among only a few[50] reported five-coordinate cobalt superoxo adducts in the literature. Classic studies in cobalt dioxygen reactivity were predominantly focused on six-coordinate products, which also coordinate oxygen reversibly, but in contrast are accessible in high conversion.[72,75] The reported octahedral complexes are characterized as low-spin cobalt(III) species, with the unpaired electron residing on the superoxo moiety. The five-coordinate superoxo complexes reported here likewise have unpaired electron density on the superoxo moiety, as judged by EPR spectroscopy. In contrast to the octahedral systems, DFT analysis here indicates that the $S = 2$ cobalt spin state is favored, albeit only by 3 kcal mol^{-1} (within the accuracy of the calculation). This electronic structure requires that the d_{z^2} orbital—or σ^* orbital for the Co−O_2 bond—is partially occupied. The σ-bonding interaction is thus rather weak, and this is likely the origin of the positive $\Delta G°$ for dioxygen binding. In related systems, Borovik et al. have shown that tripodal cobalt complexes with hydrogen-bond donor groups in the second-coordination sphere react with dioxygen to generate $Co^{III}OH$ products through an unknown pathway.[50,82] The difference in the reactivity to $[\mathbf{Co(TN^{Bn})}]^-$ could be ascribed to the different nature of the pendant group (hydrogen-bond donor vs acceptor), the proximity of the pendant group, the electron density at the metal center, or steric accessibility of the open coordination site.

We originally targeted a tripodal ligand design as a promising modular system that would lead to improved electrocatalysts of the ORR and perhaps other proton−electron reactions. We succeeded in preparing tripodal complexes that contain an open coordination site with noncoordinating amine functionalities, to facilitate proton transfer. However, the addition of 3 equiv of [H-DMF]OTf to each of the cobalt or zinc complexes generated the fully protonated pro-ligands $\mathbf{H_3(TN^{Bn})}$ or $\mathbf{H_3(TEt)}$ in quantitative yield (Scheme 7). Protonation occurs at the amide groups rather than the pendant amines, even

Scheme 6. Reversible Coordination of Dioxygen to $[\mathbf{Co(TN^{Bn})}]^-$ and $[\mathbf{Co(TEt)}]^-$, Generating Cobalt(III) Superoxo Products

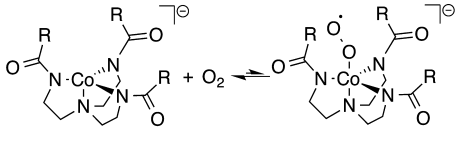

dx.doi.org/10.1021/ic5013389 | Inorg. Chem. 2014, 53, 9242−9253

Scheme 7. Instability of the Tripodal Complexes $[M(L)]^-$ to a Total of 1 and 3 equiv of Acid

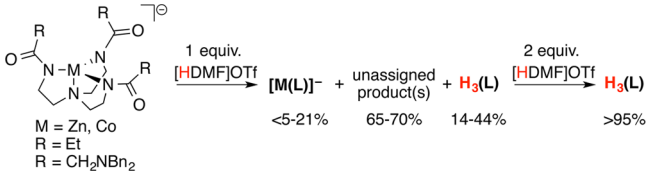

though the amide groups are coordinated to the metal center in $[M(L)]^-$. This protonation location even appears to hold for the stoichiometric addition of a single proton, in which ^{1}H NMR analysis indicated that 14−44% H_3L is generated (Table S2 in the SI). In all cases, the amide moiety rather than the pendant tertiary amine is the preferred site of protonation. Even use of weaker acids results in protonation of the amide moiety. This is a serious problem because the normal conditions for dioxygen reduction require that the acid substrate be present in large excess to the catalyst.

The monoanionic pyridyl ligand was synthesized in an effort to decrease the basicity of the nitrogen donors in the primary-coordination sphere of a resulting metal complex. The attenuated basicity of pyridine relative to amide was expected to limit complex decomposition by proteolysis with excess acid. Unfortunately, attempts thus far to generate $[M(py_2N^{Bn})]^+$ (M = Zn, Co, Fe) have been unsuccessful.

It was anticipated that protonation of the pendant base(s) in $[Co(TN^{Bn})]^-$ would increase the affinity of the complex for dioxygen because of the formation of intramolecular hydrogen bonds. Changes in the optical spectrum were observed upon treatment of an oxygenated solution of $[Co(TN^{Bn})]^-$ with [H-DMF]OTf at −20 °C. The resulting absorption bands are distinct from those observed upon the addition of acid to anaerobic solutions, and the final spectrum is identical when the order of the addition is reversed (i.e., acid and then dioxygen). However, warming the solution to room temperature resulted in decomposition, which underscores the instability of this complex to the conditions required for the ORR.

The combination of a low equilibrium constant for dioxygen binding and poor acid stability severely limits the utility of $[Co(TN^{Bn})]^-$ or $[Co(TEt)]^-$ for electrocatalysis of the ORR. Still, these ligands could be useful for catalysis. The remarkable tripodal molybdenum complexes developed by Schrock for catalytic dinitrogen reduction show similar sensitivity to excess acid.[83,84] In this case, catalytic turnover is achieved by the slow addition of an insoluble acid using a syringe pump and utilizing a chemical reductant.

CONCLUSIONS

Four entries in a new family of modular tripodal ligands have been synthesized for applications in proton−electron reactions such as the ORR. The pro-ligand $H_3(TN^{Bn})$ was designed to contain a pendant tertiary amine that could participate in proton-transfer events, a functionality that positively influences both rate and selectivity in related catalytic systems. An analogue without a pendant basic functionality, $H_3(TEt)$, was prepared as a control for reactivity studies. Cobalt(II) and zinc(II) complexes of these ligands were prepared, and all species assumed the desired coordinatively unsaturated trigonal-monopyramidal coordination mode in both the solution and solid state. However, the cobalt complexes only bind dioxygen to a very small extent. More critically, ^{1}H NMR analysis of the diamagnetic zinc analogues reveals that the complexes are not stable to acidic conditions and undergo M-L proteolysis.

This study reveals that the tripodal ligand family reported here is not a suitable framework to identify relationships between the primary/secondary-coordination sphere structure and catalyst performance (e.g., rate, selectivity, overpotential). Future ligand design should balance the requirements of modularity, for systematic structure variation, with the basicity of the primary-coordination sphere. The reactivity of the coordinating groups with added acid is a serious problem in the design of ligands with pendant, nonbinding acid/base groups. The $P_2^RN_2^{R'}$ ligands avoid this problem because they bind to relatively soft metal centers with soft donor ligands, leaving the harder amine ligands available to bind to the hard proton. However, soft donors are not typically compatible with the oxidative conditions of the ORR. When hard donors are needed, there is a concern that the basicity of these donors will be greater than the pendant base groups, leading to ligand displacement from the metal in the presence of protons. The "hangman" porphyrin and corrole ligands developed by Nocera, and our pyridyl and carboxyphenyl porphyrin examples, prevent protonation of the metal-coordinating groups and binding of the potential proton relays through the rigidity of the ligand framework. The strategy of kinetically inhibiting protonation of the primary-coordination sphere through more rigid ligand structures is worth probing further.

EXPERIMENTAL SECTION

Synthesis of H_3(TEt). Tris(2-aminoethyl)amine (tren; 1.392 g, 9.519 mmol) was combined with NEt_3 (3.855 g, 0.03810 mol) in CH_2Cl_2 (20 mL) under dinitrogen and cooled in an ice bath. Propionyl chloride (3.524 g, 0.03809 mmol) was added dropwise. A white solid ($HNEt_3Cl$) formed immediately, and an additional portion of CH_2Cl_2 (20 mL) was added to facilitate stirring. The reaction was allowed to warm to room temperature and was stirred for 21 h. Filtration removed some of $HNEt_3Cl$. The remainder of the salt was removed through successive crystallizations from CH_2Cl_2 and a final crystallization from acetone. The solvent from the final crystallization was removed, and the resulting oil was purified by column chromatography [4% methanol (MeOH) in CH_2Cl_2] with silica (neutralized with 1% NEt_3 in CH_2Cl_2). The purified product slowly solidified to a white solid over 1 day. Yield: 1.133 g (38%). RF = 0.24 in 10% MeOH in CH_2Cl_2. ^{1}H NMR ($CDCl_3$, 499 MHz): δ 6.79 (br s, 3H, N*H*), 3.26−3.25 (m, 6H, NCH_2CH_2NH), 2.53 (m, 6H, NCH_2CH_2NH), 2.23 (q, J = 5.0 Hz, 6H, $COCH_2CH_3$), 1.12 (t, J = 5.0 Hz, 9H, $COCH_2CH_3$). ^{13}C NMR ($CDCl_3$, 126 MHz): δ 174.8 (s, $NHC(O)CH_2$), 54.6 (s, NCH_2CH_2NH), 37.7 (s, NCH_2CH_2NH), 29.5 (s, $COCH_2CH_3$), 10.0 (s, $COCH_2CH_3$). HR-MS. Calcd ($[M + Na]^+$): m/z 337.2215. Obsd: m/z 337.2209. IR (KBr pellet, cm^{-1}): 3284 [br s, ν(NH)], 1653 [s, ν(CO)].

Synthesis of (Dibenzylamino)acetic Acid Methyl Ester. Glycine methyl ester hydrochloride (6.072 g, 48.40 mmol) and $NaHCO_3$ (24.397 g, 290.42 mmol) were combined with dimethyl sulfoxide (DMSO; 25 mL) and tetrahydrofuran (THF; 180 mL) in a round-bottomed flask. Benzyl bromide (25.661 g, 150.03 mmol) was added, followed by THF (20 mL), and the reaction was stirred at 60 °C for 19 h. The reaction was filtered and washed with THF. The filtrate was collected, and the solution was concentrated under vacuum. Water (20 mL) was added, and the pH was increased to 9. The mixture was extracted with CH_2Cl_2 (3 × 25 mL). The organic layers were combined and dried with $MgSO_4$, and the solvent was removed under vacuum to afford a yellow oil. The pure product (RF = 0.24; 10% MeOH in CH_2Cl_2) was obtained by column chromatography (0−2% EtOAc in hexanes) using neutralized silica (1% NEt_3 in hexanes). Yield: 11.189 g (86%). ^{1}H NMR ($CDCl_3$, 499 MHz): δ

dx.doi.org/10.1021/ic5013389 | Inorg. Chem. 2014, 53, 9242−9253

7.43−7.41 (m, 4H, *Ph*), 7.36−7.33 (m, 4H, *Ph*), 7.29−7.26 (m, 2H, *Ph*), 3.84 (s, 4H, NCH_2Ph), 3.71 (s, 3H, OCH_3), 3.33 (s, 2H, C(O)CH_2N). ^{13}C NMR ($CDCl_3$, 126 MHz): δ 172.0 (s, OC(O)-CH_2), 139.1 (s, *Ph*), 129.0 (s, *Ph*), 128.4 (s, *Ph*), 127.3 (s, *Ph*), 57.9 (s, NCH_2Ph), 53.5 (s, C(O)CH_2N), 51.4 (s, OCH_3). HR-MS. Calcd ([M + H]$^+$): *m*/*z* 270.1494. Obsd: *m*/*z* 270.1501. IR (KBr pellet, cm^{-1}): 1749 [s, ν(CO)].

***N*,*N*-Dibenzylglycine Hydrochloride.** A solution of (dibenzylamino)acetic acid methyl ester (10.4413 g, 38.7656 mmol) in MeOH (120 mL) was cooled in an ice bath. LiOH (9.289 g, 388.0 mmol) dissolved in water (120 mL) was slowly added to the MeOH solution. The reaction was allowed to warm to room temperature and was then heated to 60 °C for 18 h. The reaction was cooled, and HCl (64 mL, 6 M) was added to bring the pH to 3. At this point, the product hydrochloride salt precipitated as a white powder. The powder was filtered, washed with C_6H_6 (2 × 15 mL) and Et_2O (3 × 15 mL), and dried. A second crop of product precipitated from the filtrate. This solid was filtered, washed with water (2 × 10 mL), C_6H_6 (2 × 10 mL), and Et_2O (2 × 15 mL), and dried. The combined yield was 10.2033 g (90%). The ^{1}H NMR spectrum of the product matched literature values.[85]

Synthesis of H_3(TN^{Bn}). *N*,*N*-Dibenzylglycine hydrochloride (5.021 g, 17.21 mmol) was added to a 250 mL flask under dinitrogen, followed by CH_2Cl_2 (15 mL) and NEt_3 (1.915 g, 18.92 mmol, 1.1 equiv). The hydrochloride salt became mostly soluble within 10 min. To the reaction was added *N*-hydroxysuccinimide (NHS; 2.969 g, 25.80 mmol, 1.5 equiv), 1-ethyl-3-[3-(dimethylamino)propyl]-carbodiimide hydrochloride (EDAC; 4.946 g, 25.80 mmol, 1.5 equiv), and CH_2Cl_2 (20 mL), and the reaction was stirred for 24 h. Tren (856 mg, 5.73 mmol, 0.33 equiv) was added to the clear yellow reaction, and the solution was stirred for 6 days. The reaction was extracted with pH 9 NaOH (2 × 10 mL) and water (10 mL). The aqueous layer was neutralized and extracted with CH_2Cl_2 (3 × 10 mL). The combined organic layers were washed with brine (15 mL) and dried with $MgSO_4$, and the solvent was removed under vacuum. The pure product (RF = 0.49; 10% MeOH in CH_2Cl_2) was obtained by column chromatography (4% MeOH in CH_2Cl_2) using neutralized silica (1% NEt_3 in CH_2Cl_2). Yield: 4.12 g (84%). ^{1}H NMR ($CDCl_3$, 499 MHz): δ 7.32−7.20 (m, 33H, *Ph* and N*H*CO), 3.59 (s, 12H, NCH_2Ph), 3.21 (m, 6H, NCH$_2$CH_2NH), 3.10 (s, 6H, COCH_2N), 2.52 (t, *J* = 5.0 Hz, 6H, NCH_2CH$_2$NH). ^{13}C NMR ($CDCl_3$, 126 MHz): δ 171.3 (s, NHC(O)CH$_2$), 138.0 (s, *Ph*), 129.0 (s, *Ph*), 128.7 (s, *Ph*), 127.7 (s, *Ph*), 59.3 (s, NCH$_2$Ph), 57.5 (s, NCH$_2$CH$_2$NH), 53.3 (s, C(O)CH$_2$N), 36.9 (s, NCH$_2$CH$_2$NH). HR-MS. Calcd ([M + H]$^+$): *m*/*z* 858.5071. Obsd: *m*/*z* 858.5066. IR (KBr pellet, cm^{-1}): 3370 [m, ν(NH)], 1669 [s, ν(CO)].

Synthesis of H_3(TN^{Ph}). 2-(*N*-Methyl-*N*-phenylamino)benzoic acid (2.190 mg, 9.636 mmol), NHS (2.441 mg, 21.21 mmol), and EDAC (4.070 g, 21.21 mmol) were added to a reaction flask and placed under nitrogen, and CH_2Cl_2 (50 mL) was added to the reactants. The solution was stirred at room temperature for 6 h. An aqueous solution of $NaHCO_3$ (35 mL) was added to the reaction and extracted with CH_2Cl_2 (3 × 40 mL). The combined organic layers were dried with $MgSO_4$ and filtered, and the volatile solvents were evaporated under vacuum to afford a yellow solid (84% of isolated yield). The product was dried further by washing with diethyl ether (3 × 10 mL) and drying under vacuum (18 h). A solution of the dried product (500 mg, 1.54 mmol) in CH_2Cl_2 (70 mL) was added to a solution of tren (75 mg, 0.51 mmol) in CH_2Cl_2 (2 mL). The reaction was stirred at 40 °C for 3 h, after which the volatile solvents were evaporated under vacuum to afford a light-brown solid. The crude product was purified by column chromatography (3% MeOH in CH_2Cl_2) with neutralized silica (washed with 1% NEt_3 in CH_2Cl_2). The product **H_3(TN^{Ph})** was isolated as an off-white solid. Yield: 355 mg (76% over two steps). ^{1}H NMR ($CDCl_3$, 301 MHz): δ 8.20−8.08 (m, 6H, *Ar* and N*H*CO), 7.47−7.39 (m, 3H, *Ar*), 7.36−7.28 (m, 3H, *Ar*), 7.16−7.07 (m, 9H, *Ar*), 3.13−3.08 (m, 15H, NCH$_2$CH_2NH and NCH_3Ph), 2.34 (t, *J* = 6.0 Hz, 6H, NCH_2CH$_2$NH). ^{13}C NMR ($CDCl_3$, 126 MHz): δ 166.1 (s, C(O)NH), 149.1 (s, *Ar*), 147.9 (s, *Ar*), 132.6 (s, *Ar*), 131.4 (s, *Ar*), 131.3 (s, *Ar*), 129.2 (s, *Ar*), 127.9 (s, *Ar*), 126.6 (s, *Ar*), 119.8 (s, *Ar*), 115.8 (s, *Ar*), 52.8 (s, NCH$_2$CH$_2$NH), 40.8 (s, NCH$_3$Ph), 37.4 (s, NCH$_2$CH$_2$NH). HR-MS. Calcd ([M + H]$^+$): *m*/*z* 774.4132. Obsd: *m*/*z* 774.8. IR (KBr pellet, cm^{-1}): 3383 [m, ν(NH)], 1653 [s, ν(CO)].

Synthesis of H(py$_2$N^{Bn}). *N*,*N*-Dibenzylglycine hydrochloride (433 mg, 1.48 mmol) was added to a 250 mL flask under dinitrogen, followed by CH_2Cl_2 (200 mL) and NEt_3 (220 mg, 2.16 mmol, 1.46 equiv). The hydrochloride salt became soluble within 10 min. To the reaction was added hydroxybenzotriazole (227 mg, 1.48 mmol, 1.0 equiv). The reaction was cooled to 0 °C in an ice bath, and dicyclohexylcarbodiimide (DCC; 306 mg, 1.48 mmol, 1.0 equiv) was added as a solution in CH_2Cl_2 (5 mL). After 15 min, (2-aminoethyl)bis(2-pyridylmethyl)amine (300 mg, 1.23 mmol, 0.83 equiv) was added, and the reaction was allowed to warm to room temperature. After stirring for 72 h, a white precipitate had formed on top of the solution. The solids are byproducts from the coupling reaction (including a DCC hydration product, dicyclohexylurea) that are partially soluble in CH_2Cl_2. The solvent was removed, and MeCN (50 mL) was added to fully precipitate the byproducts. The solution was filtered through Celite, the filtrate was dried with Na_2SO_4, and the solvent was removed under vacuum. The pure product (RF = 0.27; 2.5% MeOH in CH_2Cl_2) was obtained as a yellow oil by column chromatography (2.5% MeOH in CH_2Cl_2) using alumina (Fluka, pH 9.5) as the stationary phase. Yield: 200 mg (34%). ^{1}H NMR ($CDCl_3$, 500 MHz): δ 8.56 (d, *J* = 4 Hz, 2H, py-*H*), 7.60 (br s, 1H, N*H*COCH$_3$), 7.54 (m, 2H, py-H), 7.43 (m, 2H, py-H), 7.38 (m, 4H, Ph-H), 7.28 (m, 6H, Ph-H), 7.16 (m, 2H, py-H), 3.87 (s, 4H, pyCH_2N), 3.66 (s, 4H, PhCH_2N), 3.40 (m, 2H, NCH$_2$CH_2NH), 3.15 (s, 2H, COCH_2NBn$_2$), 2.77 (t, *J* = 5.3 Hz, 2H, NCH_2CH$_2$NH). ^{13}C NMR ($CDCl_3$, 500 MHz): δ 170.0 (s, NHC(O)CH$_2$), 159.0 (s, *Ar*), 149.0 (s, *Ar*), 138.0 (s, *Ar*), 136.0 (s, *Ar*), 129.0 (s, *Ar*), 128.0 (s, *Ar*) 127.0 (s, *Ar*) 123.0 (s, *Ar*), 122.0 (s, *Ar*), 60.0 (s, pyCH$_2$N), 59.0 (s, NCH$_2$Ph), 57.0 (s, NCH$_2$CH$_2$NH), 53.0 (s, C(O)CH$_2$N), 36.0 (s, NCH$_2$CH$_2$NH). HR-MS. Calcd ([M + H]$^+$): *m*/*z* 480.2673. Obsd: *m*/*z* 480.27. IR (solution, CCl_4, cm^{-1}): 1589 [m, ν(CO)].

General Procedure for the Synthesis of K[M(L)]. Synthesis of K[Zn(TEt)]. The pro-ligand **H_3(TEt)** (216 mg, 0.688 mmol) was dissolved in DMF (3 mL) and added to solid KH (110 mg, 2.75 mmol). Dihydrogen bubbles evolved immediately. The reaction was left to stir at room temperature for 7 h. Zn(OAc)$_2$ (126 mg, 0.688 mmol) was added, and DMF (1 mL) was used to wash the solid into the reaction vial. The reaction was stirred again at room temperature for 11 h. The resulting pale-yellow suspension was filtered, and the solid K(OAc) was washed with DMF (3 × 1 mL). The combined washings were concentrated to ca. 1−2 mL, and to this was added Et_2O (4 mL). The resulting suspension was cooled to −10 °C to promote further precipitation. The resulting solid was isolated by filtration and purified by successive washes with THF (3 mL), MeCN (3 mL), and Et_2O (3 mL). Yield: 138 mg (48%). ^{1}H NMR (DMF-d_7, 500 MHz): δ 3.32 (t, *J* = 5 Hz, C(O)NCH_2, 6H), 2.56 (t, *J* = 5 Hz, C(O)NCH$_2$CH_2N, 6H), 2.13 (q, *J* = 5 Hz, CH_2CH$_3$, 6H), 1.07 (t, J = 5 Hz, CH$_2$CH_3, 9H). ^{13}C{^{1}H} NMR (DMF-d_7, 126 MHz): δ 176.2 (s, NC(O)Et), 53.0 (s, C(O)NCH$_2$CH$_2$N), 42.9 (s, C(O)NCH$_2$CH$_2$N), 35.1 (s, CH$_2$CH$_3$), 12.2 (s, CH$_2$CH$_3$). IR (KBr pellet, cm^{-1}): 1665 [s, ν(C═O)], 1569 [s, ν(C═O)]. MALDI MS (pyrene matrix): Calcd ([**Zn(TEt)**]$^-$): *m*/*z* 375.1. Obsd: *m*/*z* 375.3.

Characterization of K[Zn(TN^{Bn})]. Yield: 102 mg (29%). ^{1}H NMR (DMF-d_7, 499 MHz): δ 7.18−7.39 (m, Ar-*H*, 30H), 3.61 (s, NCH_2Ph, 12H), 3.36 (m, C(O)NCH_2CH$_2$, 6H), 3.14 (s, C(O)CH_2N, 6H), 2.53 (m, C(O)NCH$_2$CH_2N, 6H). ^{13}C{^{1}H} NMR (CD_3CN, 126 MHz): δ 173.3 (s, C(O)N), 141.7 (s, Ar), 130.4 (s, Ar), 129.4 (s, Ar), 128.0 (s, Ar), 62.8 (s, CH$_2$), 58.8 (s, CH$_2$), 54.6 (s, CH$_2$), 42.7 (s, CH$_2$). IR (KBr pellet, cm^{-1}): 1675 [s, ν(C═O)], 1576 [s, ν(C═O)]. MALDI MS (pyrene matrix): Calcd ([**Zn(TNBn)**]$^-$): *m*/*z* 918.4. Obsd: *m*/*z* 918.5.

K[Co(TEt)]. Yield: 116 mg (39%).

K[Co(TN^{Bn})]. Yield: 176 mg (43%).

General Procedure for the Synthesis of NEt$_4$[Co(L)]. Synthesis of NEt$_4$[Co(TEt)]. A solution of NEt_4Cl (47 mg, 0.28 mmol) in CH_3CN (4 mL) was added to solid **K[Co(TEt)]** (116 mg, 0.283 mmol). The suspension was stirred at room temperature for 3 days.

dx.doi.org/10.1021/ic5013389 | *Inorg. Chem.* 2014, 53, 9242−9253

The reaction was filtered to obtain KCl as a white solid and the product $NEt_4[Co(TEt)]$ as a blue filtrate. The filtrate was concentrated to ca. 2 mL and passed through a microfiber glass filter plug to remove any residual KCl, and Et_2O (12 mL) was added to the solution. Pure product slowly crystallized after cooling to −10 °C. Combining metalation with cation exchange is feasible; however, these reactions consistently resulted in lower overall purity. This is due to the similar relative solubilities of $NEt_4[Co(L)]$ and any contaminating ligand, which hinders reprecipitation or crystallization attempts. Yield: 45 mg (38%). ^{1}H NMR (CD_3CN, 499 MHz): δ 90.02 (br s), 84.05 (br s), 3.35 (s, NCH_2CH_3, 8H), 1.37 (s, NCH_2CH_3, 12H), −0.98 (br s). μ_B (Evans' method, DMF-d_7, 298 K): μ_{eff} = 4.36. IR (KBr pellet, cm^{-1}): 1676 [m, ν(C═O)], 1655 [m, ν(C═O)], 1558 [s, ν(C═O)]. UV [1:1 THF/DMF; λ_{max}, nm (ε, M^{-1} cm^{-1})]: 404 (30), 584 (100), 609 (93). X-band EPR (1:1 THF/DMF): 77 K, g = 3.78; 10 K, $g_\perp$ = 4.28, $g_\parallel$ = 2.00 ($A_z = 96 \times 10^{-4}$ cm^{-1}). MALDI MS (pyrene matrix): Calcd ($[Co(TEt)]^-$): m/z 370.1. Obsd: m/z 370.2.

Characterization of $NEt_4[Co(TN^{Bn})]$. Yield: 173 mg (39%). ^{1}H NMR (CD_3CN, 499 MHz): δ 78.78 (br), 6.81 (br s), 6.00 (br s), 5.25 (br s), 3.27 (br s, NCH_2CH_3, 8H), 1.30 (br s, NCH_2CH_3, 12H), −6.05 (br s). μ_B (Evans' method, DMF-d_7, 298 K): μ_{eff} = 4.21. IR (KBr pellet, cm^{-1}): 1675 [s, ν(C═O)], 1576 [s, ν(C═O)]. UV [1:1 THF/DMF; λ_{max} nm (ε, M^{-1} cm^{-1})]: 412 (31), 588 (104), 614 (103). X-band EPR (1:1 THF/DMF, 20 mM): 77 K, g = 3.83; 10 K, $g_\perp$ = 4.30, $g_\parallel$ = 2.00 ($A_z = 98 \times 10^{-4}$ cm^{-1}). MALDI MS (pyrene matrix): Calcd ($[Co(TNBn)]^-$): m/z 913.4. Obsd: m/z 913.5.

■ ASSOCIATED CONTENT

Supporting Information

X-ray crystallographic data in CIF format, additional experimental details (including procedures for reactivity studies), computational details, NMR, IR, and MALDI MS spectra, UV−vis and ^{1}H NMR titration data, and additional XRD tables. This material is available free of charge via the Internet at http://pubs.acs.org.

■ AUTHOR INFORMATION

Corresponding Authors

*E-mail: jblacqu2@uwo.ca.
*E-mail: james.mayer@yale.edu.

Author Contributions

J.M.B. led the project and designed, prepared, and characterized the C_3-symmetric ligands and their complexes, in collaboration with A.F. M.L.P. performed all of the studies of the pyridyl ligand. S.R. performed all of the computational studies and W.K. the crystallographic studies. S.A.C. and T.T. performed and interpreted the EPR experiments. The manuscript was written through contributions of all authors. All authors have given approval to the final version of the manuscript.

Notes

The authors declare no competing financial interest.

■ ACKNOWLEDGMENTS

Drs. T. A. Tronic, M. T. Mock, Z. M. Heiden, and C. J. Weiss of the Center for Molecular Electrocatalysis and Dr. A. S. Borovik of the University of California—Irvine are thanked for helpful discussions. This research was supported as part of the Center for Molecular Electrocatalysis, an Energy Frontier Research Center funded by the U.S. Department of Energy, Office of Science, Office of Basic Energy Sciences. The National Science and Engineering Research Council of Canada is thanked for a PDF award for J.M.B.

■ REFERENCES

(1) Winter, M.; Brodd, R. J. *Chem. Rev.* **2004**, *104*, 4245.
(2) Gewirth, A. A.; Thorum, M. S. *Inorg. Chem.* **2010**, *49*, 3557.
(3) Savéant, J.-M. *Chem. Rev.* **2008**, *108*, 2348.
(4) DuBois, D. L.; Bullock, R. M. *Eur. J. Inorg. Chem.* **2011**, *2011*, 1017.
(5) Rakowski Dubois, M.; Dubois, D. L. *Acc. Chem. Res.* **2009**, *42*, 1974.
(6) Helm, M. L.; Stewart, M. P.; Bullock, R. M.; DuBois, M. R.; DuBois, D. L. *Science* **2011**, *333*, 863.
(7) Wiese, S.; Kilgore, U. J.; Ho, M.-H.; Raugei, S.; DuBois, D. L.; Bullock, R. M.; Helm, M. L. *ACS Catal.* **2013**, *3*, 2527.
(8) Mock, M. T.; Chen, S.; O'Hagan, M.; Rousseau, R.; Dougherty, W. G.; Kassel, W. S.; Bullock, R. M. *J. Am. Chem. Soc.* **2013**, *135*, 11493.
(9) Yang, J. Y.; Bullock, R. M.; Dougherty, W. G.; Kassel, W. S.; Twamley, B.; DuBois, D. L.; Rakowski DuBois, M. *Dalton Trans.* **2010**, *39*, 3001.
(10) Tronic, T. A.; Rakowski DuBois, M.; Kaminsky, W.; Coggins, M. K.; Liu, T.; Mayer, J. M. *Angew. Chem., Int. Ed.* **2011**, *50*, 10936.
(11) Tronic, T. A.; Kaminsky, W.; Coggins, M. K.; Mayer, J. M. *Inorg. Chem.* **2012**, *51*, 10916.
(12) McGuire, R., Jr.; Dogutan, D. K.; Teets, T. S.; Suntivich, J.; Shao-Horn, Y.; Nocera, D. G. *Chem. Sci.* **2010**, *1*, 411.
(13) Dogutan, D. K.; Stoian, S. A.; McGuire, R.; Schwalbe, M.; Teets, T. S.; Nocera, D. G. *J. Am. Chem. Soc.* **2011**, *133*, 131.
(14) Carver, C. T.; Matson, B. D.; Mayer, J. M. *J. Am. Chem. Soc.* **2012**, *134*, 5444.
(15) Matson, B. D.; Carver, C. T.; Von Ruden, A.; Yang, J. Y.; Raugei, S.; Mayer, J. M. *Chem. Commun.* **2012**, *48*, 11100.
(16) Collman, J. P.; Wagenknecht, P. S.; Hutchison, J. E. *Angew. Chem., Int. Ed.* **1994**, *33*, 1537.
(17) Chang, C. K.; Liu, H. Y.; Abdalmuhdi, I. *J. Am. Chem. Soc.* **1984**, *106*, 2725.
(18) Halime, Z.; Kotani, H.; Li, Y.; Fukuzumi, S.; Karlin, K. D. *Proc. Natl. Acad. Sci. U. S. A.* **2011**, *108*, 13990.
(19) Boulatov, R.; Collman, J. P.; Shiryaeva, I. M.; Sunderland, C. J. *J. Am. Chem. Soc.* **2002**, *124*, 11923.
(20) Rosenthal, J.; Nocera, D. G. *Acc. Chem. Res.* **2007**, *40*, 543.
(21) Kadish, K. M.; Shen, J.; Frémond, L.; Chen, P.; Ojaimi, M. E.; Chkounda, M.; Gros, C. P.; Barbe, J.-M.; Ohkubo, K.; Fukuzumi, S.; Guilard, R. *Inorg. Chem.* **2008**, *47*, 6726.
(22) Askarizadeh, E.; Yaghoob, S. B.; Boghaei, D. M.; Slawin, A. M. Z.; Love, J. B. *Chem. Commun.* **2010**, *46*, 710.
(23) Devoille, A. M. J.; Love, J. B. *Dalton Trans.* **2012**, *41*, 65.
(24) Collman, J. P.; Boulatov, R.; Sunderland, C. J.; Fu, L. *Chem. Rev.* **2004**, *104*, 561.
(25) Holm, R. H.; Kennepohl, P.; Solomon, E. I. *Chem. Rev.* **1996**, *96*, 2239.
(26) Thorseth, M. A.; Letko, C. S.; Tse, E. C. M.; Rauchfuss, T. B.; Gewirth, A. A. *Inorg. Chem.* **2013**, *52*, 628.
(27) Jones, M. B.; MacBeth, C. E. *Inorg. Chem.* **2007**, *46*, 8117.
(28) Das, U. K.; Bobak, J.; Fowler, C.; Hann, S. E.; Petten, C. F.; Dawe, L. N.; Decken, A.; Kerton, F. M.; Kozak, C. M. *Dalton Trans.* **2010**, *39*, 5462.
(29) Searls, C. E.; Kleespies, S. T.; Eppright, M. L.; Schwartz, S. C.; Yap, G. P. A.; Scarrow, R. C. *Inorg. Chem.* **2010**, *49*, 11261.
(30) Harman, W. H.; Harris, T. D.; Freedman, D. E.; Fong, H.; Chang, A.; Rinehart, J. D.; Ozarowski, A.; Sougrati, M. T.; Grandjean, F.; Long, G. J.; Long, J. R.; Chang, C. J. *J. Am. Chem. Soc.* **2010**, *132*, 18115.
(31) Ward, A. L.; Elbaz, L.; Kerr, J. B.; Arnold, J. *Inorg. Chem.* **2012**, *51*, 4694.
(32) Fukuzumi, S.; Kotani, H.; Lucas, H. R.; Doi, K.; Suenobu, T.; Peterson, R. L.; Karlin, K. D. *J. Am. Chem. Soc.* **2010**, *132*, 6874.
(33) Shook, R. L.; Peterson, S. M.; Greaves, J.; Moore, C.; Rheingold, A. L.; Borovik, A. S. *J. Am. Chem. Soc.* **2011**, *133*, 5810.
(34) Moore, C. M.; Quist, D. A.; Kampf, J. W.; Szymczak, N. K. *Inorg. Chem.* **2014**, *53*, 3278.
(35) Moore, C. M.; Szymczak, N. K. *Dalton Trans.* **2012**, *41*, 7886.

(36) Sickerman, N. S.; Park, Y. J.; Ng, G. K. Y.; Bates, J. E.; Hilkert, M.; Ziller, J. W.; Furche, F.; Borovik, A. S. *Dalton Trans.* **2012**, *41*, 4358.
(37) Park, Y. J.; Sickerman, N. S.; Ziller, J. W.; Borovik, A. S. *Chem. Commun.* **2010**, *46*, 2584.
(38) Matsumoto, J.; Suzuki, T.; Kajita, Y.; Masuda, H. *Dalton Trans.* **2012**, *41*, 4107.
(39) Szajna-Fuller, E.; Chambers, B. M.; Arif, A. M.; Berreau, L. M. *Inorg. Chem.* **2007**, *46*, 5486.
(40) Berreau, L. M. *Eur. J. Inorg. Chem.* **2006**, *2006*, 273.
(41) Lee, J. H.; Park, J.; Lah, M. S.; Chin, J.; Hong, J.-I. *Org. Lett.* **2007**, *9*, 3729.
(42) Metteau, L.; Parsons, S.; Mareque-Rivas, J. C. *Inorg. Chem.* **2006**, *45*, 6601.
(43) Rivas, J. C. M.; Hinchley, S. L.; Metteau, L.; Parsons, S. *Dalton Trans.* **2006**, 2316.
(44) Matson, E. M.; Bertke, J. A.; Fout, A. R. *Inorg. Chem.* **2014**, *53*, 4450.
(45) Lacy, D. C.; Mukherjee, J.; Lucas, R. L.; Day, V. W.; Borovik, A. S. *Polyhedron* **2013**, *52*, 261.
(46) Ng, G. K. Y.; Ziller, J. W.; Borovik, A. S. *Chem. Commun.* **2012**, *48*, 2546.
(47) Parsell, T. H.; Yang, M.-Y.; Borovik, A. S. *J. Am. Chem. Soc.* **2009**, *131*, 2762.
(48) Mukherjee, J.; Lucas, R. L.; Zart, M. K.; Powell, D. R.; Day, V. W.; Borovik, A. S. *Inorg. Chem.* **2008**, *47*, 5780.
(49) Shook, R. L.; Borovik, A. S. *Chem. Commun.* **2008**, 6095.
(50) Lucas, R. L.; Zart, M. K.; Murkerjee, J.; Sorrell, T. N.; Powell, D. R.; Borovik, A. S. *J. Am. Chem. Soc.* **2006**, *128*, 15476.
(51) Borovik, A. S. *Acc. Chem. Res.* **2004**, *38*, 54.
(52) Kim, S.; Saracini, C.; Siegler, M. A.; Drichko, N.; Karlin, K. D. *Inorg. Chem.* **2012**, *51*, 12603.
(53) Syuhei, Y.; Hideki, M. *Sci. Technol. Adv. Mater.* **2005**, *6*, 34.
(54) Cheruzel, L. E.; Cecil, M. R.; Edison, S. E.; Mashuta, M. S.; Baldwin, M. J.; Buchanan, R. M. *Inorg. Chem.* **2006**, *45*, 3191.
(55) Wada, A.; Yamaguchi, S.; Jitsukawa, K.; Masuda, H. *Angew. Chem., Int. Ed.* **2005**, *44*, 5698.
(56) Yamaguchi, S.; Wada, A.; Funahashi, Y.; Nagatomo, S.; Kitagawa, T.; Jitsukawa, K.; Masuda, H. *Eur. J. Inorg. Chem.* **2003**, *2003*, 4378.
(57) Alliger, G. E.; Müller, P.; Cummins, C. C.; Nocera, D. G. *Inorg. Chem.* **2010**, *49*, 3697.
(58) Smith, N. D.; Wohlrab, A. M.; Goodman, M. *Org. Lett.* **2005**, *7*, 255.
(59) Kim, Y. K.; Lee, S. J.; Ahn, K. H. *J. Org. Chem.* **2000**, *65*, 7807.
(60) Silverstein, R. M.; Webster, F. X.; Kiemle, D. J. *Spectrometric Identification of Organic Compounds*, 7th ed.; John Wiley & Sons: Hoboken, NJ, 2005.
(61) Suzuki, T.; Imai, K.; Nakagawa, H.; Miyata, N. *ChemMedChem* **2006**, *1*, 1059.
(62) Schatz, M.; Leibold, M.; Foxon, S. P.; Weitzer, M.; Heinemann, F. W.; Hampel, F.; Walter, O.; Schindler, S. *Dalton Trans.* **2003**, 1480.
(63) Several samples of $[\mathbf{Co(L)}]^-$ were analyzed by elemental analysis, and all were slightly outside the accepted level of error. We do not attribute the deviation to a systematic impurity given that the magnitude and type (i.e., %C vs %H) of error were not consistent across the samples.
(64) Niklas, N.; Wolf, S.; Liehr, G.; Anson, C. E.; Powell, A. K.; Alsfasser, R. *Inorg. Chim. Acta* **2001**, *314*, 126.
(65) Girolami, G. S.; Rauchfuss, T. B.; Angelici, R. J. *Synthesis and Technique in Inorganic Chemistry: A Laboratory Manual*, 3rd ed.; University Science Books: Sausalito, CA, 1999.
(66) Ray, M.; Hammes, B. S.; Yap, G. P. A.; Rheingold, A. L.; Borovik, A. S. *Inorg. Chem.* **1998**, *37*, 1527.
(67) Eelman, M. D.; Blacquiere, J. M.; Moriarty, M. M.; Fogg, D. E. *Angew. Chem., Int. Ed.* **2008**, *47*, 303.
(68) Lacy, D. C.; Park, Y. J.; Ziller, J. W.; Yano, J.; Borovik, A. S. *J. Am. Chem. Soc.* **2012**, *134*, 17526.
(69) Drago, R. S. *Physical Methods for Chemists*, 2nd ed.; Surfside Scientific Publishers: Gainesville, FL, 1992.
(70) Pfaff, F. F.; Kundu, S.; Risch, M.; Pandian, S.; Heims, F.; Pryjomska-Ray, I.; Haack, P.; Metzinger, R.; Bill, E.; Dau, H.; Comba, P.; Ray, K. *Angew. Chem., Int. Ed.* **2011**, *50*, 1711.
(71) Drago, R. S.; Corden, B. B. *Acc. Chem. Res.* **1980**, *13*, 353.
(72) Tovrog, B. S.; Kitko, D. J.; Drago, R. S. *J. Am. Chem. Soc.* **1976**, *98*, 5144.
(73) Izutsu, K. *Acid–Base Dissociation Constants in Dipolar Aprotic Solvents*; Blackwell Scientific: Oxford, U.K., 1990.
(74) Kaljurand, I.; Kütt, A.; Sooväli, L.; Rodima, T.; Mäemets, V.; Leito, I.; Koppel, I. A. *J. Org. Chem.* **2005**, *70*, 1019.
(75) Jones, R. D.; Summerville, D. A.; Basolo, F. *Chem. Rev.* **1979**, *79*, 139.
(76) Drago, R. S.; Cannady, J. P.; Leslie, K. A. *J. Am. Chem. Soc.* **1980**, *102*, 6014.
(77) To the best of our knowledge, ϵ values for trigonal-bipyramidal cobalt(III) superoxo complexes are not available. We use a typical value here for related octahedral species to obtain a rough estimate of K_{eq} for dioxygen coordination in the systems reported herein.
(78) Zhao, Y.; Truhlar, D. G. *J. Chem. Phys.* **2006**, *125*.
(79) Radoń, M.; Pierloot, K. *J. Phys. Chem. A* **2008**, *112*, 11824.
(80) Ali, M. E.; Sanyal, B.; Oppeneer, P. M. *J. Phys. Chem. B* **2012**, *116*, 5849.
(81) Smith, T. D.; Pilbrow, J. R. *Coord. Chem. Rev.* **1981**, *39*, 295.
(82) MacBeth, C. E.; Hammes, B. S.; Young, V. G.; Borovik, A. S. *Inorg. Chem.* **2001**, *40*, 4733.
(83) Yandulov, D. V.; Schrock, R. R. *Science* **2003**, *301*, 76.
(84) Schrock, R. R. *Acc. Chem. Res.* **2005**, *38*, 955.
(85) Breitenmoser, R. A.; Heimgartner, H. *Helv. Chim. Acta* **2001**, *84*, 786.

dx.doi.org/10.1021/ic5013389 | *Inorg. Chem.* 2014, 53, 9242–9253